Int. J. Electrochem. Sci., 7 **(2012)** 9881 - 9891

International Journal of
ELECTROCHEMICAL
SCIENCE
www.electrochemsci.org

Gaseous and Electrochemical Hydrogenation Properties of $LaNi_{4.3}(Co, Al)_{0.7-x}In_x$ Alloys

K. Giza[1], *H. Bala*[1], *H. Drulis*[2,*], *A. Hackemer*[2], *L. Folcik*[2]

[1] Czestochowa University of Technology, Faculty of Materials Processing, Technology and Applied Physics, Al. Armii Krajowej 19, 42-200 Częstochowa, Poland
[2] Trzebiatowski Institute of Low Temperatures and Structure Research PAS, Okolna Str.2 P.O.Box 1410, 50-950 Wrocław, Poland
[*]E-mail: h.drulis@int.pan.wroc.pl

Received: 26 July 2012 / *Accepted:* 6 September 2012 / *Published:* 1 October 2012

In this paper the effect of indium on the hydrogenation behaviour of the $LaNi_{4,3}(Co, Al)_{0.7-x}$ In_x (x = 0, 0.1, 0.2, 0.3) alloys at room temperature is presented. The pressure–composition (*p–c*) measurements show that the highest hydrogen concentration of 1.68 wt.% is reached for indium-free (x = 0) alloy. The partial substitution of Al or Co by In causes a slight diminishing of maximum hydrogen concentration. Indium decreases also the plateau hydrogen equilibrium pressure from p_{eq} = 0.37 bar (In-free alloy) to p_{eq} = 0.06 bar (for $LaNi_{4.3}Co_{0.2}In_{0.2}Al_{0.3}H_y$) hydride. The electrochemical performance of the studied alloys were characterized using dc. polarization techniques. Electrochemical galvanostatic hydrogenation experiments at 60 mA/g discharge rate revealed the largest discharge current capacity of 305 mAh/g for $LaNi_{4.3}Co_{0.4}Al_{0.2}In_{0.1}$ alloy. The hydrogen discharge capacity evidently drops with total substitution of aluminium by indium. There is no significant difference in the discharge potentials for the tested electrodes. The relative diffusion coefficient of hydrogen (D/a^2) varies in the range of (1.2 to 3.5) $\cdot 10^{-5}$ s^{-1}.

Keywords: hydrogen storage alloys, *p-c* isotherms, charge/discharge curves.

1. INTRODUCTION

Hydrogen storage alloys (HSA) are a group of materials which can be used in the rechargeable metal hydride (Ni-MH) batteries. Materials suitable for the above applications should be characterized by a high hydrogen capacity, moderate hydride stability and reasonably fast hydrogen absorption/desorption processes. The HSA should also demonstrate a nearly constant equilibrium pressure during a solid phase conversion (MH_α to MH_β). The information about these characteristics is

commonly derived from the pressure-composition, (*p-c*) isotherms [1,2] and electrochemical charge/discharge measurements [3,4]. At present, the commercialized hydrogen storage electrode materials are mainly AB_5-type alloys, which usually display a capacities of 300–330 mAh/g. Many methods such as optimization of composition, doping of different elements and adoption of non-stoichiometric composition were applied to improve both the HSA discharge capacity and cycle life [5]. However, the beneficial effect of the substituents for either La or Ni is often accompanied by undesirable decrease in hydrogen absorption capacity, long activation and low rate of hydrogen absorption/desorption process. In our recent paper [6] we described the hydrogenation properties of $La_{0.5}RE_{0.5}Ni_{4.8}Al_{0.1}Li_{0.1}$ (RE = Ce, Pr or Nd) alloys. Partial substitution of La with Ce, Pr or Nd in the $LaNi_{4.8}Al_{0.1}Li_{0.1}$ alloy causes the decrease of the hydrogen capacity and an increase of the hydrogen equilibrium pressure. As it has been reported in literature [7-9], Al partial substitution for Ni decreases the plateau pressure but evidently impairs the hydrogen storage capacity. Van Mal et al [10] investigated the hydrogen absorption of $LaNi_{5-x}Co_x$ alloys and found that partial replacement of nickel by cobalt decreased the equilibrium pressure. Unfortunately, the increasing cobalt content distinctly decreases maximum absorption capacity of the alloys. It was reported that the addition of In to lanthanum-based HSA caused the expansion of unit cell volume and increased point defect density in the alloys [11,12]. In our previous report [13] we evaluated electrochemical properties of the $LaNi_{3.6}(Co,Mn,Al)_{1.2}In_{0.2}$ type alloys and we have found that partial substitution of Co, Mn or Al by In caused decrease of both exchange current density of H_2O/H_2 system and current capacity of the electrode materials. We also investigated electrochemical properties of the $LaNi_{5-x}In_x$ (x = 0.1, 0.2 and 0.5) alloys [14] and found that the maximum discharge capacity of the alloys decreased from 319 mAh/g (x=0.1) to 239 mAh/g (x = 0.5). However, we found that partial substitution of Ni by In in $LaNi_5$ compound caused distinct decrease of the H_2 equilibrium pressure which makes them very interesting materials to be used as negative MH electrodes in the Ni/MH batteries. In the present paper we are aimed at identifying the effect of the In additive on the hydrogenation properties of $LaNi_{4,3}(Co, Al, In)_{0,7}$ alloys, which are being considered as negative electrodes in Ni-MH type batteries [15,16].

2. EXPERIMENTAL

The alloys studied in this paper, with the general chemical formula of $LaNi_{4.3}(Co, Al,)_{0.7-x}In_x$ (x = 0, 0.1, 0.2, 0.3) were prepared in an arc-furnace under high-purity argon atmosphere. The purity of all used metals was higher than 99.9 wt.%. The ingots were being turned over and remelted at least three times for homogeneity. Additionally, the alloys were annealed in an induction furnace at 850^{o}C for 4 h under vacuum (about 10^{-3}torr). The annealed alloys were mechanically crushed and ground to powder for the X-ray powder diffraction (XRD) and electrochemical measurements. The hydrogen storage properties were evaluated using a Sievert-type apparatus. Prior to hydrogen absorption and *p-c* measurements, the alloys were activated by heating to 250^{O}C under a vacuum of 10^{-3} torr for at least 2 h to remove the impurities. Then, the alloys were hydrided under a hydrogen pressure of 20 bar and dehydrided to pressure less than 0.05 bar. The amount of hydrogen absorbed by the samples was determined volumetrically. The *p-c* measurements were carried out after the samples activation (3

absorption/desorption hydrogen cycles). The desorption pressure-composition (*p-c*) isotherm measurements were carried out at room temperature (23^{o}C).

Hydride electrodes were prepared by rolling of 85% corresponding alloy powders, 10% PVDF and 5% acetylene carbon black into pellets 0.4 - 0.5 mm thick. Alloy powders were obtained by hydrogen decrepitation and their initial granulation was on the order of 1 - 100 μm. The average grain size was not possible to evaluate with satisfactory accuracy, since greater powder particles had cracks and fissures and their number increased as a result of cycling. The electrochemical charge/discharge tests were carried out in a conventional three electrode cell, consisting of a metal hydride working electrode, a reference saturated calomel electrode (SCE) and a Pt wire counter electrode, using a CHI 1140 A (Austin, Texas) workstation. The electrolyte was Ar-saturated, 6M KOH solution at a temperature of 23±0.2^{o}C. The electrodes were charged at a current density of 185 mA/g for 2 h and discharged at 60 mA/g to the anodic potential of −0.6 V (vs SCE). The chronopotentiometric discharge technique was applied to determine the relative hydrogen diffusion coefficients of the hydrogen saturated $LaNi_{4.3}(Co, Al, In)_{0.7}$ electrodes.

3. RESULTS AND DISCUSSION

The tested alloys can be roughly divided into two groups, namely (i) $LaNi_{4.3}Co_{0.4}Al_{0.3-x}In_x$ (x = 0, 0.1, 0.2, 0.3) and (ii) $LaNi_{4.3}(Co_{0.4-x}In_x)Al_{0.3}$ (x = 0.0, 0.1, 0.2). Partial (x = 0.1, 0.2) substitution of In for Al in the $LaNi_{4.3}Co_{0.4}Al_{0.3}$ compound leads to monophase alloys (solid solutions) with the hexagonal $CaCu_5$-type structure. However, in case aluminium is fully substituted by indium (x = 0.3) the X-ray diffraction pattern indicates that the sample ($LaNi_{4.3}Co_{0.4}In_{0.3}$ alloy) consists of more than only one phase. The corresponding XRD patterns are shown in Fig. 1.

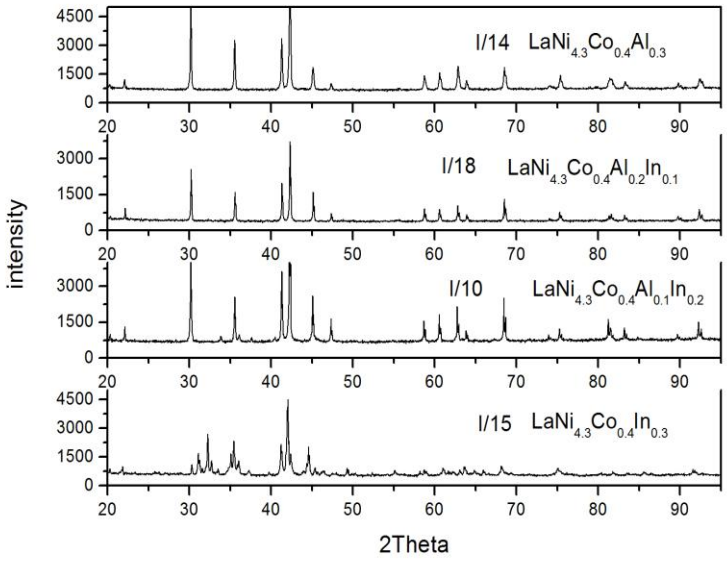

Figure 1. X-ray powder diffraction patterns (KαCu radiation) of the $LaNi_{4.3}Co_{0.4}$ $Al_{0.3-x}$ In_x samples (x = 0, 0.1, 0.2, 0.3).

3.1 Pressure-composition isotherm studies

The pressure–composition (*p*–*c*) curves of hydrogen desorption at room temperature (23^{o}C) are presented in Figs. 2 and 3. Some characteristic parameters estimated from the *p* – *c* curves are collected in Table 1.

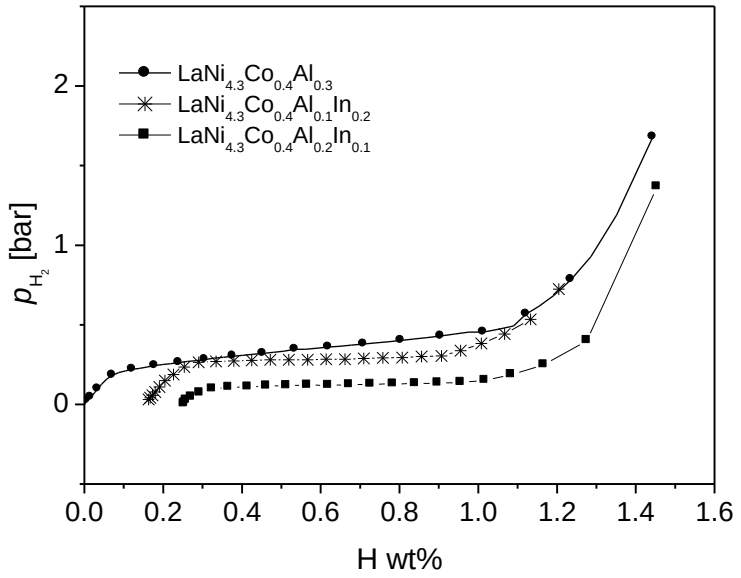

Figure 2. p–c room temperature isotherms for hydrogen desorption of $LaNi_{4.3}Co_{0.4}Al_{0.3-x}In_x$ (x = 0, 0.1, 0.2) alloys.

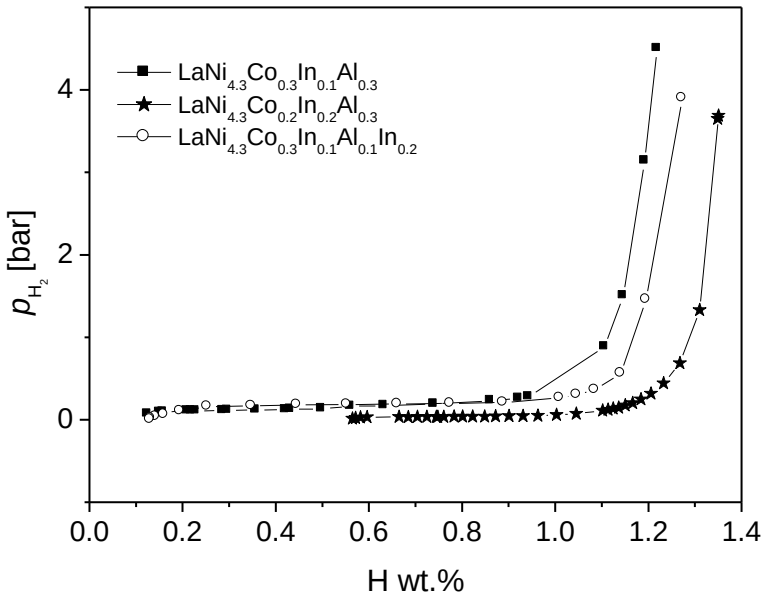

Figure 3. p–c room temperature isotherms for hydrogen desorption of $LaNi_{4,3}(Co, Al)_{0.7-x}In_x$ (x = 0.1, 0.2 , 0.3) alloys

Under hydrogen pressure of 10 bar the largest hydrogen concentration, w = 1.68 wt.%**,** has been reached for In-free composition (x = 0). The increase of In content in the Al position is prone to gradual decrease of hydrogen concentration to w = 1.45 wt.% (for x = 0.1) and w = 1.20 wt.% (for x = 0.2).

Table 1. Hydrogenation parameters of the tested $LaNi_{4.3}(Co, Al)_{0.7-x}In_x$ alloys determined from the p-c measurements (23^{o}C).

Alloy chemical formula	Maximum hydrogen concentration (w_{max})	Reversible hydrogen capacity (w_{rev})	H_2 plateau equillibrium pressure (p_{eq})
	[wt. %]	[wt. %]	[bar]
$LaNi_{4.3}Co_{0.4}Al_{0.3}$	1.68	1.03	0.37
$LaNi_{4.3}Co_{0.4}Al_{0.2}In_{0.1}$	1.45	0.83	0.12
$LaNi_{4.3}Co_{0.4}Al_{0.1}In_{0.2}$	1.20	0.81	0.27
$LaNi_{4.3}Co_{0.4}In_{0.3}$	1.38	0.77	0.72
$LaNi_{4.3}Co_{0.3}In_{0.1}Al_{0.3}$	1.22	0.94	0.19
$LaNi_{4.3}Co_{0.3}In_{0.1}Al_{0.1}In_{0.2}$	1.27	1.01	0.19
$LaNi_{4.3}Co_{0.2}In_{0.2}Al_{0.3}$	1.35	0.67	0.06

As it is shown in Table 1, the Co substitution by small amount of In (x = 0.1) decreases the maximum hydrogen concentration to w_{max} = 1.22 wt.% but larger substitution (x = 0.2) increases it to 1.35 wt.%. From the hydrogen storage properties point of view, the most important parameter is a *reversible hydrogen capacity* (RHC). The RHC is the amount of hydrogen gas reversibly released during isothermal desorption. The RHC of the alloy depends on a few factors, involving its crystal structure, phase composition and structure, grain size, composition uniformity, surface state, etc. The RHC hydrogen capacity values shown in the Table 1 were estimated from the width of plateau part of *p-c* isotherms. The longer and more horizontal the pressure plateau, the more advantageous storage characteristics of the alloy. The accuracy of measurements of the plateau width (in wt.% units) depends on the level of plateau pressure and, in particular, on the sensitivity of the bottom range of the used pressure gauge. In our case the pressure transducer used for the measurements would registered hydrogen pressure values not lower than 0.05 bar. Because of comparatively low plateau pressures for the most of studied alloys, the values of reversible capacities given in Table 1 can be underestimated. It seems, the more correct results for RHC are possible to determine from the discharge current capacity analysis in electrochemical experiments (see further parts of the paper).

The equilibrium pressures for hydrogen desorption presented in Table 1 were read in the middle of plateau. As it results from Table 1, the Al substitution by small amount of indium (x = 0.1) is prone to a decrease of the plateau pressure (p_{eq} = 0.12 bar), however, greater substitutions distinctly

increase it (p_{eq} =0.72 bar for x = 0.3). In case the cobalt is substituted by indium, the drop of plateau pressure is dramatic: from p_{eq} = 0.37 bar (for In-free alloy) to p_{eq} = 0.06 bar (for alloy with x = 0.2).

3.2 Electrochemical characterization

The changes of electrochemical discharge capacity (Q) of the tested $LaNi_{4.3}(Co,Al)_{0.7-x}In_x$ electrodes *vs* cycle number are presented in Fig. 4. As it is seen from Fig. 4, the discharge capacities of the alloys practically settle down on a constant level after 3-4 cycle.

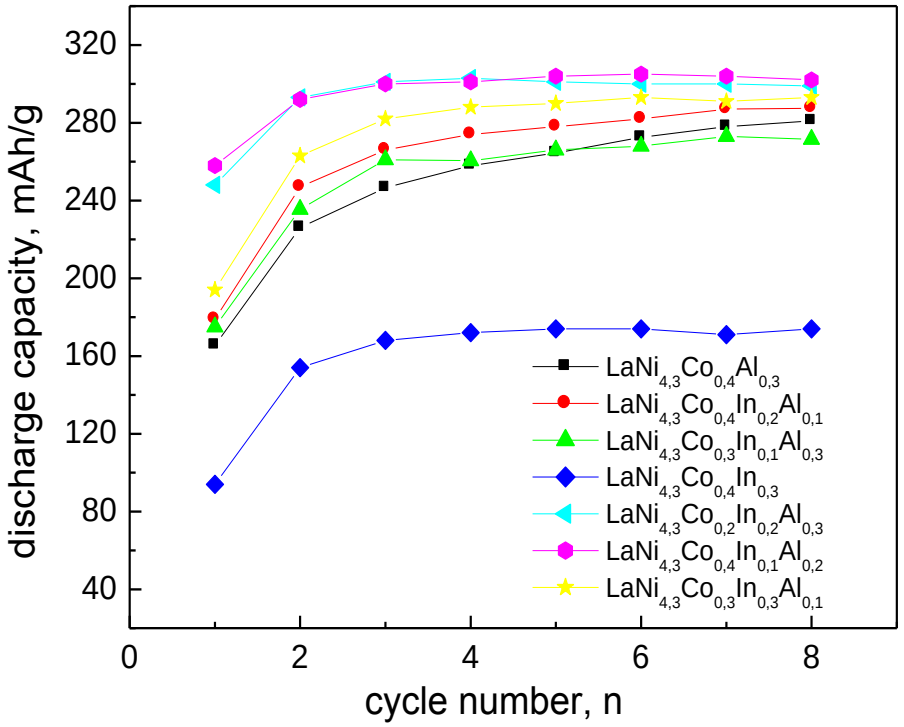

Figure 4. Discharge capacity (at anodic current 60 mA/g) of the tested alloys as a function of cycle number (Ar, 6M KOH, 23^{o}C).

Some of tested alloys reveal for Q a slight tendency to decrease with further cycling but some of them seem not to reach a maximum value even after 8th cycle. The number of hydrogen atoms which are absorbed by the compound formula unit (M is a simplified symbol of AB_5 type alloy) is equal to

$$y = \frac{Q_{max} M_M}{F} \qquad (1)$$

where Q_{max} is a maximum discharge capacity (expressed in mAh/g), M_M is the molar mass of the applied compound and F is Faraday constant, equal to 96500 A s mol^{-1} = 26806 mAh mol^{-1}. The hydrogen capacity expressed as hydrogen concentration (wt %) in the alloy is equal to

$$w = \frac{1.098 \cdot Q}{M_{MH_y}} \quad (2)$$

where M_{MH_y} is the molar mass of the hydride phase. The Q_{max} discharge capacities and corresponding concentrations of hydrogen (wt %) as well as relative effective hydrogen diffusion coefficients determined for the alloys from electrochemical experiments are listed in Table 2.

Table 2. Results of electrochemical measurements of the tested $LaNi_{4,3}(Co, Al,)_{0,7-x}$ In_x HSA

Alloy chemical formula	Maximum discharge capacity		D/a^2
	Q_{max}	w	
	[mAh/g]	[wt. %]	[s^{-1}]
$LaNi_{4.3}Co_{0.4}Al_{0.3}$	289	1.07	$1.3 \cdot 10^{-5}$
$LaNi_{4.3}Co_{0.4}Al_{0.2}In_{0.1}$	305	1.13	$2.5 \cdot 10^{-5}$
$LaNi_{4.3}Co_{0.4}Al_{0.1}In_{0.2}$	292	1.09	$2.2 \cdot 10^{-5}$
$LaNi_{4.3}Co_{0.4}In_{0.3}$	174	0.65	$1.2 \cdot 10^{-5}$
$LaNi_{4.3}Co_{0.3}In_{0.1}Al_{0.3}$	280	1.04	$1.8 \cdot 10^{-5}$
$LaNi_{4.3}Co_{0.3}In_{0.1}Al_{0.1}In_{0.2}$	293	1.09	$3.5 \cdot 10^{-5}$
$LaNi_{4.3}Co_{0.2}In_{0.2}Al_{0.3}$	303	1.12	$3.3 \cdot 10^{-5}$

There appears from data in Table 2 that the Q_{max} capacities of indium substituted, $LaNi_{4.3}Co_{0.4}Al_{0.3}$ based alloys are generally comparable (*ca* 280 – 300 mAh/g or *ca* 1.04 – 1.13 wt.%). When aluminium is fully substituted by indium, the calculated discharge capacity is distinctly smaller: *ca* 170 mAh/g and 0.65 wt.%, respectively. . The observed phenomenon results from phase structure of the tested alloys. As it can be seen from XRD patterns presented in Fig.1., the $LaNi_{4.3}Co_{0.4}In_{0.3}$ sample is a multiphase material. The distinct drop in the calculated hydrogen stoichiometric index compared to its corresponding value for monophase sample indicates that there exist some quantity of impurity phases in the alloy structure that absorb hydrogen irreversibly. These results are in good agreement with those found in *p-c* measurements (compare w values in Table 2 with w_{rev} in Table 1).

When Ni-MH batteries are applied to electric vehicles (EVs) the discharge potential of MH electrode is considered to be particularly important property, because the discharge potential determines the specific power of EVs [17]. More negative value of discharge potential leads to higher

specific power of the battery. In Fig. 5 the changes of hydrogenated electrode potentials measured at i_a = 60 mA/g *vs* discharge time of the tested alloys are shown. It can be seen that each discharge curve can be divided into two regions. Initially, the discharge process is controlled by charge transfer as indicated by a potential plateau. After a certain period of time, a drastic decrease of potential occurs due to the depletion of hydrogen atoms from the electrode surface [18]. For the $LaNi_{4.3}Co_{0.4}In_{0.3}$ alloy electrode the width of the discharge potential plateau decreases distinctly in comparison with the other six electrodes. The Co substitution by small amount of In (x = 0.1) increases insignificantly the potential at half discharge time. Moreover, a flat discharge profile is characteristic for these alloys which can be ascribed to fast hydrogen transport across the electrode. Only the $LaNi_{4.3}Co_{0.4}In_{0.3}$ alloy reveals rather unstable discharge potential. Thus, indium partial substitutions for Co and Al ensure not only stable discharge performance but also high specific power of a Ni-MH battery.

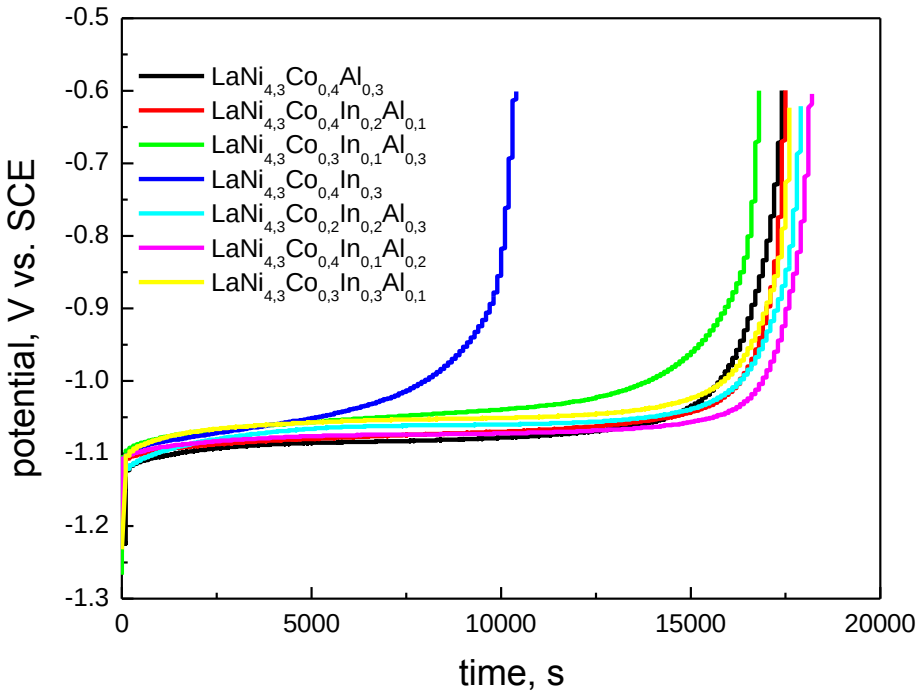

Figure 5. Galvanostatic discharge curves for the tested $LaNi_{4,3}(Co, Al)_{0,7-x}\ In_x$ electrodes at 60 mA/g discharge current density measured for 8th cycle.

In order to study hydrogen transport rate within the hydrogenated electrode, the conventional chronopotentiometric method has been widely used [19-21]. However, for a constant flux at the surface and uniform concentration of hydrogen in the bulk of the alloy, the value of relative effective diffusion coefficient ($\overline{D}/a^2$ where a is an average alloy particle radius) may be evaluated with satisfactory accuracy using the following simplified equation [22]:

$$\frac{\bar{D}}{a^2} = \frac{1}{15\left(\frac{Q_o}{i_a} - \tau\right)} \quad (3)$$

where Q_o is the capacity of the charged electrode, i_a is the applied discharge (anodic) current density and τ is the transient (discharge) time**,** i.e., the time when the hydrogen surface concentration approaches zero. Another words, the ratio Q_o/i_a corresponds to the discharge time necessary to discharge completely the electrode under hypothetical conditions when the discharge process proceeds without interference of diffusion [23]. In the absence of any other oxidation processes, the discharge process carried out at a constant current should establish a constant hydrogen flux condition [23].

In order to evaluate the diffusion coefficient using Eq. 3 it is necessary to estimate the capacity of the charged electrode (Q_o) and transient time (τ). According to our numerous experiments [24,25], the capacity of the charged electrode can be expressed as follows:

$$Q_o = i_c\, t_{ch} \quad (4)$$

where, i_c is charging current density and t_{ch} is time necessary for saturation of the electrode with atomic hydrogen. In practice, after t_{ch}, the tested electrode takes on values typical for cathodically polarized H_2O/H_2 system and generation of H_2 bubbles on the electrode surface takes place. In Fig. 6, the graphical ways of determination of t_{ch} (Fig. 6a) and τ (Fig. 6b) are visually presented.

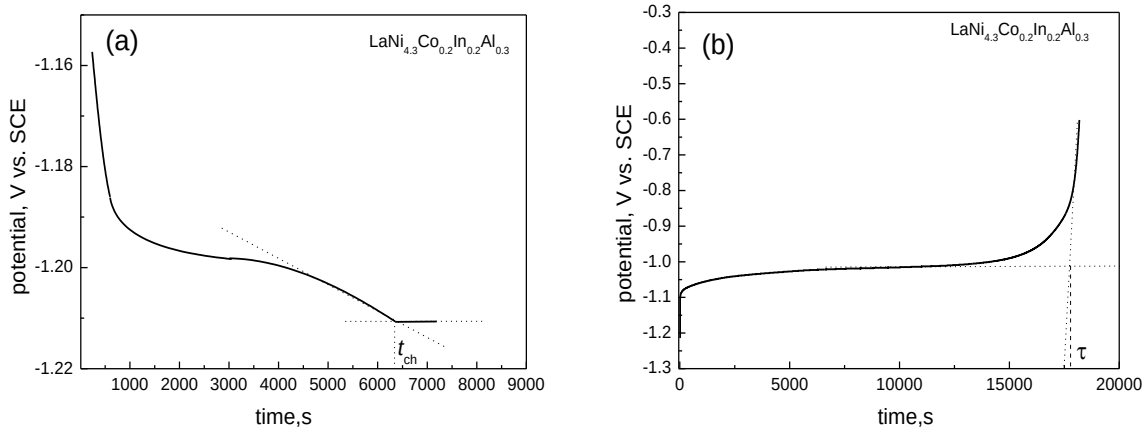

Figure 6. Galvanostatic charge (a) and discharge (b) curves for $LaNi_{4.3}Co_{0.2}In_{0.2}Al_{0.3}$ electrode and visual presentation of t_{ch} and τ determination method.

After the t_{ch} period of time the electrode potential settles down on a constant level (corresponding to the H_2O/H_2 system) and hydrogen bubbles start to evolute on the electrode surface. As it is shown in Fig. 6b, after the transition time τ, a drastic potential jump occurs to compensate the

hydrogen surface concentration decreasing and start undesirable electrode material oxidation in order to keep a constant current.

Because, it is hard to determine the real average particle size (and, thus its mean diameter *a*) of the powdered alloy obtained by hydrogen decrepitation, we use D/a^2 fraction to evaluate hydrogen diffusivity within the alloy. The calculated values of D/a^2 (we name them "relative effective diffusion coefficients") are listed in the last column of Table 2. As it can be seen, the D/a^2 values determined from the galvanostatic measurements are on the order of 10^{-5} s^{-1}. Similar D/a^2 values for the hydrogen diffusivity were also determined by Zheng et al [19] and Zhao et al **[**26] in the AB_5 – type alloys.

4. CONCLUSIONS

Indium substitution for Co and Al in $LaNi_{4,3}(Co, Al,)_{0,7-x}In_x$ compound modifies the alloy hydrogenation behavior - it causes distinct decrease of the H_2 equilibrium pressure. From the application point of view, the lowering of hydrogen pressure is a positive tendency, enabling its use in battery applications. Unfortunately, the lower equilibrium pressure is achieved by the cost of reduced hydride capacity. The tested alloys reveal acceptably high current capacities (280-305 mAh/g after 4-5 charge/discharge cycles) which practically does not change with several further cycles. For $LaNi_{4.3}Co_{0.4}In_{0.3}$ alloy the discharge capacity is clearly less: 174 mAh/g only. The relative hydrogen diffusion coefficients in the tested alloys are of the level of (1.2 to 3.5) 10^{-5} s^{-1}.

ACKNOWLEDGEMENTS
The research was supported by Wrocław Research Centre EIT + under the project "The Application of Nanotechnology in Advanced Materials" - NanoMat (*POIG.01.01.02-02-002/08)* financed by the European Regional Development Fund (*Innovative Economy Operational Programme,* 1.1 .2*)*

References

1. J. Kleperis, G. Wójcik, A. Czerwiński, J. Skowroński, M. Kopczyk and M. Bełtowska-Brzezińska, *J. Solid State Electrochem*. 5 (2001) 229
2. I. P. Jain and M. I. S. Abu Dakka, *Int. J. Hydrogen Energy* 22 (1997) 1117
3. F. Feng and D. O. Nortwood, J. *Power Sources* 136 (2004) 346
4. S. Li, M. Zhao, L. Wang, Y. Liu and Y. Wang, *Mat. Science Eng. B*, 150 (2008) 168
5. Y. Q. Lei, J. J. Jiang, D. L. Sun, J . Wu and Q. D. Wang, *J Alloys Compd*., 231 (1995) 553
6. K. Giza, W. Iwasieczko, H. Bala, V. V. Pavlyuk and H. Drulis; *Int. J. Hydrogen Energy* 34 (2009) 913
7. E. Anil Kumar, M. Prakash Maiya, S. Srinivasa Murthy and B. Viswanathan, *J. Alloys. Compd*. 476 2009) 92
8. K. Giza, W. Iwasieczko, V. V. Pavlyuk, H. Bala, H. Drulis and L. Adamczyk, *J. Alloys Compd*. 429 (2007) 352
9. K. Sakaki, E. Akiba, M. Mizuno, H. Araki and Y. Shirai, *J. Alloys Compd*. 473 (2009) 87
10. H. H. van Mal, K. H. J. Buschow and F. A. Kuijpers, *J. Less-Common Met*. 32 (1973) 289
11. M. H. Mendelsohn and D. M. Gruen, *Mat. Res. Bull*. 13 (1978) 1221
12. A. Drašner and Z. Blažina, *J. Alloys Compd*. 420 (2006) 213

13. L. Adamczyk, K. Giza, H. Drulis, H. Bala and A. Hackemer, *Ochr. przed Korozją* 55 (2012) 182
14. H. Drulis, K. Giza, A. Hackemer, L. Folcik, Ł. Gondek, H. Figiel and H. Bala; *Bulletin of the Polish Hydrogen and Fuel Cell Association* 6 (2011) 115
15. N. Kuriyama, T. Sakai, H. Miyamura, H. Tanaka, H.T. Takeshita and I. Uehara, *J. Alloys Compd.* 253/254 (1997) 598
16. T. Sakai, I. Uehara and H. Ishikawa, *J. Alloys Compd*. 295 (1999) 762
17. F. Feng and D.O. Northwood, *Surf. Coating Tech*. 167 (2003) 263
18. X. Zhao, Y. Ding, M. Yang and L. Ma, *Int. J. Hydrogen Energy* 33 (2008) 81
19. G. Zheng, B. N. Popov and R. E. White; *J. Electrochem. Soc.* 142 (1995) 2695
20. T. Nishina, H. Ura and I. Uchida, *J. Electrochem. Soc*. 144 (1997) 1273
21. X. G. Yang, Q. A. Zhang, K. Y. Shu, Y. L. Du, Y. Q. Lei, Q. D. Wang and W. K. Zhang, *J. Power Sources* 90 (2000) 170
22. X. Yuan and N. Xu, *J. Appl. Electrochem*. 31 (2001) 1033
23. P.N. Popov, G. Zheng and R.E. White, *J. Appl. Electrochem*. 26 (1996) 603
24. H. Bala, I. Kukuła, K. Giza, B. Marciniak, E. Różycka-Sokołowska and H. Drulis, *Int. J. Hydrogen Energy* (in press)
25. M. Dymek and H. Bala, *Ochr. przed Korozją* (in press)
26. X. Zhao, L. Ma, Y. Ding and X. Shen, *Int. J. Hydrogen Energy* 34 (2009) 3389

© 2012 by ESG (www.electrochemsci.org)